Exo-zodi detection capability of the Ground-Based European Nulling Interferometry Experiment (GENIE) Instrument

Oswald Wallner, Reinhold Flatscher, and Klaus Ergenzinger

The *Ground-Based European Nulling Interferometry Experiment* (GENIE) is intended as an Earth-based precursor for the European Darwin mission that will prepare the Darwin science program and demonstrate the required technology at system level. We propose a compact nulling interferometer design consisting of a two-telescope aperture configuration, an optional split-pupil add-on, and only four active control loops for counteracting environmentally induced disturbances. We show by simulation that the proposed instrument is able to detect, within a few minutes of observation time, exo-zodiacal dust clouds around Sunlike stars at 20 parsecs that are 20 times stronger than the local zodiacal dust cloud density.

OCIS codes: 350.1270, 120.3180, 120.4640.

1. Background

The objective of the European Darwin mission[1] is to detect and analyze terrestrial exoplanets orbiting Sunlike stars (F, G, or K type). The technique of nulling interferometry[2] allows for visual detection and interferometric imaging of such planets. The requirements on the instruments are challenging due to the small angular separation between star and planet and the huge contrast ratio, even in the midinfrared. Further instrumental challenges are caused by the large operational bandwidth of 6.5 to 20 μm. This bandwidth is determined by the scientific goal of spectroscopically observing absorption lines of biomarkers as methane (7–8 μm), ozone (9.6 μm), carbon dioxide (15 μm and around 18 μm), and water (6–8 μm and 17–20 μm).

A nulling interferometer provides both high on-axis light suppression and high angular resolution. In the simplest arrangement, the sum of star and planet waves is received by two identical telescopes. One of the resulting signals is subject to a phase change of π, and both signals are superimposed to obtain interference. The starlight is strongly reduced by the (quadratic) on-axis null of the interferometer's transmission map, while the planet's light experiences constructive interference by proper adjustment of the baseline. Configurations with more than two telescopes allow for better rejection of the on-axis starlight, either due to a broader null or due to calibration by means of phase chopping.

Due to the tremendous requirements given by the Darwin mission, advanced observation techniques and a sophisticated instrument design are required together with the development of novel subsystems and optical components with so far unknown quality. The European Space Agency (ESA) has initiated system studies, a technology development program to provide the key elements, and breadboard activities to demonstrate stable nulling at laboratory conditions. The Ground-Based European Nulling Interferometry Experiment[3] (GENIE) is intended as next step toward Darwin. A nulling interferometer, implemented at the *Very Large Telescope Interferometer* (VLTI)[4] and operated in the midinfrared on astronomical targets, shall prepare the Darwin science program and shall demonstrate on ground and at system level the technology required to accomplish the scientific goals of Darwin.

2. Objectives and Requirements

The objectives of the GENIE project are twofold. From a technological and operational point of view the goal is to advance and mature the experience on

O. Wallner (oswald.wallner@astrium.eads.net), R. Flatscher, and K. Ergenzinger are with EADS Astrium GmbH, 88039 Friedrichshafen, Germany.

Received 6 May 2005; revised 6 January 2006; accepted 11 February 2006; posted 16 February 2006 (Doc. ID 61976).

0003-6935/06/184404-07$15.00/0

designing, manufacturing, and operating a nulling interferometer employing Darwin representative concepts and technologies. From a scientific point of view the goal is to perform a systematic survey of candidate targets for Darwin in order to screen out stars with too bright exo-zodiacal dust clouds.

The GENIE instrument shall be designed to demonstrate deep nulling of single stars or close binaries in a midinfrared spectral band of 10% relative bandwidth. Rejection ratios of more than 1000 shall be achieved for G- and K-type stars located within 50 pc of Earth. The instrument shall be able to detect dust clouds as strong as 20 times the solar zodiacal dust cloud and shall perform spectroscopy on the dust clouds with a spectral resolution as low as 10.

3. Proposed GENIE Instrument

Although GENIE is intended as a ground-borne precursor for Darwin, the two instruments will exhibit distinct differences imposed by the Earth's atmosphere:

- The atmospheric transmission strongly depends on the wavelength because of absorption features due to water, ozone, or carbon dioxide. Just these absorption lines, whose detection is the primary goal of Darwin, are a problem for GENIE. Only those wavelength bands may be used that provide sufficient transmission.
- The infrared background due to sky emission (caused by atmospheric absorption) and thermal emission from the instrument itself is one of the main limiting factors for Earth-based instruments. Both emit infrared radiation at about 300 K, which adds at the detector incoherently to the received scientific signals. In contrast to the star-to-planet flux ratio that decreases, the influence of background radiation increases dramatically with increasing wavelength. Originally the L' band (3.74 μm) and the N band (10.2 μm) have been considered for GENIE. We designed our instrument for operation in the L' band because of the higher achievable signal-to-noise ratio (SNR) for exo-zodi detection compared to the N band. Moreover, with the Keck Nuller,[5] the Large Binocular Telescope[6] (LBT), and the MIDI Midinfrared interferometric instrument[7] (MIDI) three interferometers for the N band are available.
- Atmospheric turbulence causes local variations of the temperature and of the air and water vapor density. The resulting refractive index fluctuations generate wavefront distortions that manifest themselves in scintillation, Strehl ratio fluctuations, optical path difference (OPD) fluctuations, and longitudinal dispersion. Unique to ground-based instruments is the required wavefront correction and longitudinal dispersion control.

The GENIE instrument shall be implemented at the VLTI where, with some mechanical restrictions, almost any combination of unit telescopes (UT) or auxiliary telescopes (AT) can be used. For the sake of maximum sensitivity, maximum starlight suppression, and therefore minimum system complexity, we propose a Bracewell nulling interferometer utilizing UT2 and UT3. This configuration has the smallest possible baseline of 46.6 m and maximum detection area of 50.3 m^2 per telescope. Figure 1 shows the corresponding transmission map, i.e., the on-sky response of the interferometer; compare Eq. (2). Dark areas correspond to low transmission and bright areas to high transmission. The circle indicates the instrument's field-of-view (FOV), i.e., that off-axis angle where the transmission drops to one-half of the maximum value.

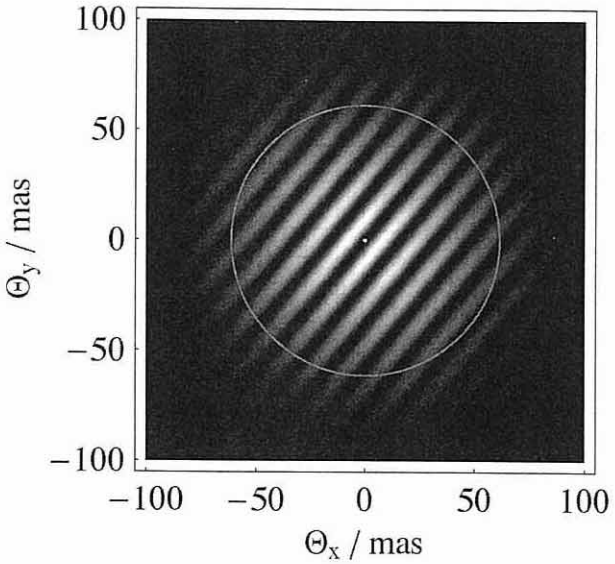

Fig. 1. Transmission map of a two-telescope nulling interferometer utilizing UT2 and UT3. The circle indicates the instrument's field of view.

The schematic instrument layout of our proposed GENIE instrument is given in Fig. 2. The core of the instrument is a fully symmetric, modified Mach–Zehnder interferometer[8] together with an achromatic phase shifter (APS). The double-pass configuration provides two identical constructive and two identical destructive outputs. Provided that the two beam-splitter plates are identical, the two destructive outputs are independent from the actual beam-splitter properties, and each output therefore provides highly symmetric superposition of the input beams. The APS is realized by a first-order system of dispersive wedges. Due to the material properties and the simple design, a maximum static OPD error of less than 2.6 nm may occur within the 10% operational bandwidth.

To achieve deep nulling of the star signal, the individual interferometer arms have to be equalized by means of modal filtering of the output signals with single-mode fibers and by active control loops counteracting intensity mismatch, OPD fluctuations, longitudinal intraband dispersion, and internal tip/tilt fluctuations. In contrast to the tip/tilt control operating in J band (1.25 μm), all other control loops operate within the scientific L' band. This has the

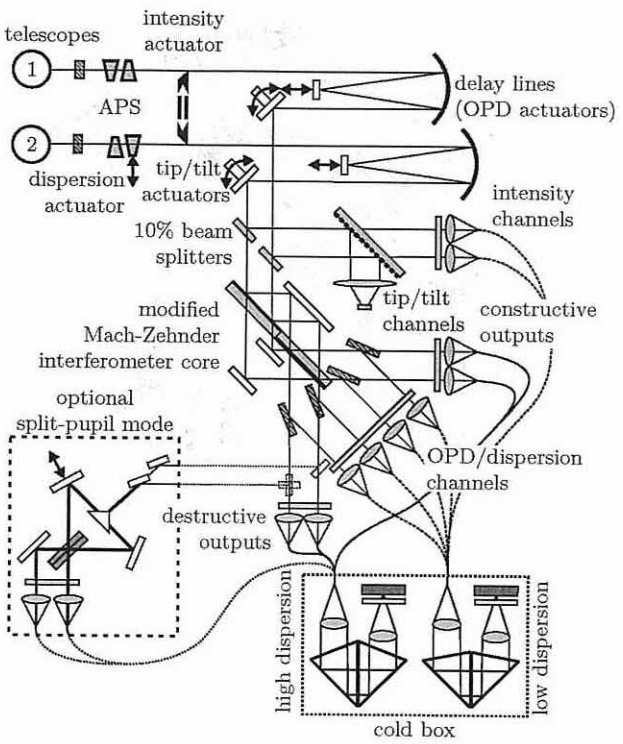

Fig. 2. Schematic layout of the proposed GENIE instrument. The two-beam setup consists of four control loops, a perfectly symmetric interferometer core providing two identical destructive outputs, and an optional split-pupil add-on allowing for background calibration.

advantage for OPD and longitudinal dispersion control that no inter band dispersion fluctuations have to be taken into account. Interband dispersion correction always suffers from strong uncertainties or from high complexity because it requires a theoretical model together with two or more fringe trackers operating at different wavelengths. Because the control signals are extracted from the science signals subsequent to the interferometer, no internal laser metrology is required. The OPD control is done by means of cat's eye delay lines, longitudinal dispersion control by acting on the dispersive wedges serving as achromatic phase shifter, tip/tilt control by actuating redirection mirrors, and intensity control by means of a beam scraper.

All signals from the scientific outputs and from the control channels are coupled into single-mode fibers that are then fed into a Dewar cooled with liquid nitrogen. The fiber output signals are dispersed by prisms on a Hawaii-1RG detector to achieve a spectral resolution of 30 for the control channels and of 400 for the science channels.

We further make use of the VLTI fringe-sensing unit PRIMA FSU (the Phase-Referenced Imaging and Microarcsecond Astronomy Facility, Fringe Sensing Unit) and of the VLTI adaptive optics system MACAO (Multiapplication Curvature Adaptive Optics).[4] However, the coarse OPD control performed by the PRIMA FSU is not mandatory.

4. GENIE Performance Prediction

The power detected at the output of an interferometer with N arms is given by

$$P = \iint_{\mathrm{FOV}} I(\theta_x,\ \theta_y) T(\theta_x,\ \theta_y) \mathrm{d}\theta_x \mathrm{d}\theta_y + P_{\mathrm{back}}, \qquad (1)$$

where I is the source intensity distribution due to star, planet, and exo-zodiacal dust cloud, T is the interferometer's transmission map, and P_{back} is the incoherent background noise power. The integration is performed over the instrument's field of view (FOV), and (Θ_x, Θ_y) are the off-axis angles in the x and y directions. The transmission map, i.e., the interferometer response on-sky, is given by

$$T(\theta_x,\ \theta_y) = \left| \sum_{n=1}^{N} M_n(\theta_x,\ \theta_y) t_n \exp\left[j \frac{2\pi}{\lambda} (x_n \theta_x + y_n \theta_y) \right] \right|^2, \qquad (2)$$

where (x_n, y_n) are the aperture-plane center coordinates of the receive telescopes, t_n are the complex transmission factors of each interferometer arm, and M_n are the individual telescope modes propagated back into the source plane. The M_n include the telescope design and the fundamental fiber mode as well as coupling into the single-mode fibers. Because the GENIE instrument provides a single spatial mode at its output, any environmental or instrumental influences can simply be taken into account by the transmission factors t_n.

The transmission factor t_n of each interferometer arm,

$$t_n = t_{n,I}\, t_{n,\mathrm{INT}}\, t_{n,\mathrm{OPD}}\, t_{n,\mathrm{LD}}, \qquad (3)$$

is the product of the deterministic instrument transmission $t_{n,I}$, the transmission factor $t_{n,\mathrm{INT}}$ due to stochastic intensity errors, the transmission factor $t_{n,\mathrm{OPD}}$ due to stochastic OPD errors, and the transmission factor $t_{n,\mathrm{LD}}$ due to differential OPD errors caused by longitudinal dispersion.

The deterministic instrument transmission, determined by the elements within the optical train, amounts to 10.1% for the science channel, to 2.1% for the intensity sensing channel, to 3.4% for the dispersion sensing channel, and to 10.1% for the OPD sensing channel. Here we assumed a minimum number of optical components, reflection factors of 99%, and transmission factors of 98%. The single-mode fiber acting as a modal wavefront filter has been assumed to be made of chalcogenide glass with a typical attenuation coefficient of 5 dB/m.

The instantaneous transmission factors are derived from the respective control loop output power spectral densities. For each control loop the output power spectral density, S_{out},

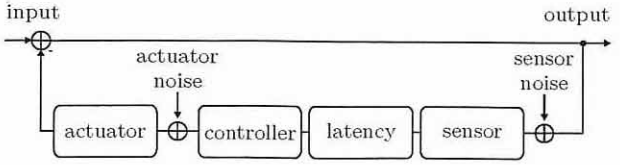

Fig. 3. Generic description of the GENIE control loops. The sensor averages the input signals within a certain period and adds some sensor noise in terms of photon noise and detector read-out noise. The multistage PID controller acts via the actuator onto the input signal. The actuator noise is assumed to be negligible. The latency takes into account any latency time occurring within the control loop.

$$S_{\mathrm{out}}(f) = \underbrace{|H_{\mathrm{CL}}(f)|^2\, S_{\mathrm{in}}(f)}_{S_{\mathrm{err}}(f)} + \underbrace{|H_{\mathrm{ST}}(f)|^2\, N_{\mathrm{S}}(f)}_{S_{\mathrm{sens}}(f)} + \underbrace{|H_{\mathrm{AT}}(f)|^2\, N_{\mathrm{A}}(f)}_{S_{\mathrm{act}}(f)} \quad (4)$$

is given by the sum of S_{err}, resulting from the input power spectral density S_{in}, S_{sens}, resulting from the sensor noise, and S_{act}, resulting from the actuator noise. The closed loop transfer function is given by H_{CL}, N_{S}, and N_{A} are the sensor noise and the actuator noise, and H_{ST} and H_{AT} are the corresponding noise transfer functions. The generic description of the control loops is given in Fig. 3. Each control loop consists of a sensor that averages the input signals within a certain period and that adds some sensor noise in terms of photon noise and detector readout noise. The controller acts via the actuator on the input signal. It is modeled as a multistage PID (proportional, integral, and derivative) controller that is optimized for each source scenario. For each stage the transfer function is given by $H(f) = K[1 + f/(jf/f_I) + jf/f_D]$, where K is the gain and f_I and f_D are the integrator and differentiator cutoff frequencies. The actuators show low-pass behavior. The transfer functions of the dispersive wedges and the beam scrapers are described by models, the transfer function of the delay line has been measured and the exact amplitude and phase distribution has been used for the simulation. The actuator noise is assumed to be negligible. For all control loops a total latency time of 25 μs has been assumed.

Figure 4 shows as an example the performance of the longitudinal dispersion control loop in terms of the power spectral density (PSD). The dashed curve gives the input PSD S_{in}, and the solid curve shows the output PSD S_{out} after correction with the control loop. The dash-dotted curve gives the output PSD S_{err} resulting from the input signal only, and the dotted curve shows the output PSD S_{sens} due to sensor noise only. The input PSD S_{in}, i.e., the PSD of the optical path difference fluctuations due to longitudinal dispersion, has been derived from the Kolmogorov model of the atmosphere[9] with parameters typical for Paranal. A gray fringe tracker is used as a sensor to measure the optical path difference. By optimizing each of the control loops for each source scenario, the residual fluctuations are minimized; see Table 1.

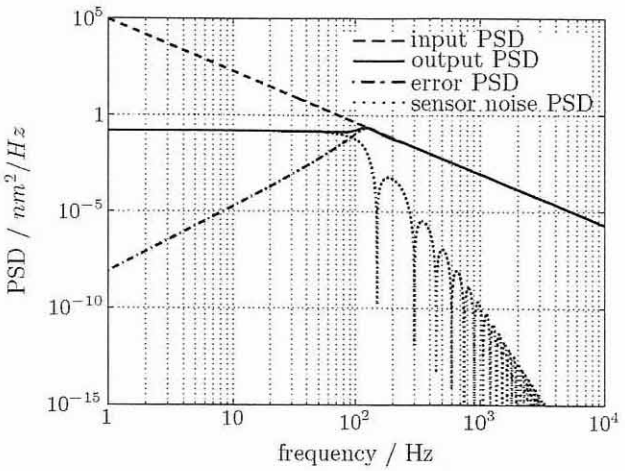

Fig. 4. Power spectral density (PSD) of the OPD fluctuations due to longitudinal dispersion before and after suppression by the GENIE dispersion control loop together with the error PSD (resulting only from the input PSD) and the sensor noise PSD.

To predict the performance of our GENIE instrument, we simulated typical observation scenarios including the following:

- A Sunlike star (G type) located almost at zenith at distances from 10 to 38 pc from Earth.
- An exo-zodiacal dust cloud seen face-on with densities from 20 to 100 times the density of the local zodiacal dust cloud. We simulated the exo-zodiacal dust cloud according to the DIRBE model[10] as the product of an emissivity function (taking into account thermal emission and scattering) and a three-dimensional dust density function.
- A hot-Jupiter planet located within the FOV, typically at an off-axis position of 0.033 astronomical units.
- Background conditions typical for the VLT site and the VLTI instrument. The emissivity of the sky as well as of the optical components of the VLTI and of the GENIE instrument are taken into account.

We simulated observations with the goal to determine the maximum achievable signal-to-noise ratio (SNR) and the time required to achieve a sufficiently high SNR. The SNR for detecting an exo-zodiacal

Table 1. GENIE Control Loop Performance in Terms of Residual rms Errors for Source Scenarios at Different Distances from Earth

rms Error	Input Error	Residual rms Error (pc) 10	20	30	38	Actuator Bandwidth
OPD (nm)	130	11.5	17.0	24.5	31.8	6 kHz
Dispersion (nm)	600	6.3	10.2	15.2	18.2	100 Hz
Intensity (%)	45	1.6	1.8	2.6	5.5	150 Hz

dust cloud is given by the ratio of the mean number $\langle Z \rangle$ of zodi photons to the noise photons,

$$\mathrm{SNR} = \langle Z \rangle / (N_{\mathrm{ph}} + N_{\mathrm{tr}} + N_{\mathrm{cal}} + N_{\mathrm{det}})^{1/2}, \quad (5)$$

where the latter consists of the following:

- Photon noise N_{ph} is caused by the stochastic nature of light.
- Transmission noise N_{tr} is caused by amplitude and phase fluctuations resulting from residual errors of the control loops which, in general, cannot perfectly eliminate the environmental perturbations. By proper design of the control loops, the transmission noise may be minimized.
- Calibration noise N_{cal} is caused by calibration uncertainties of stellar leakage and infrared background. Stellar leakage calibration is done by a model. Due to uncertainties in the measured apparent star diameter, the telescope baseline, and the wavelength, relative stellar leakage calibration errors of typically 1% seem to be realistic. The background is calibrated by virtual chopping, i.e., by measuring the background simultaneously with the science signals. Calibration errors occur because of cross coupling between the fibers used for the science signals and that used for background measurements and because of inhomogeneities of the sky background and the VLTI background. Assuming rather homogeneous background and low cross coupling, relative background calibration accuracies of 0.01% seem feasible.
- Detector noise N_{det}, i.e., dark current and read-out noise, are caused by the detector itself and depend on the type of detector used, the operational mode, and the operational conditions. For a Hawaii-1RG detector operated in the L' band, the dark current is negligible and the read-out noise is as low as a few electrons per pixel.

The maximum achievable SNR is limited by calibration noise. For infinitely long observation time the SNR for detecting an exo-zodiacal dust cloud approaches the fundamental limit

$$\mathrm{SNR}(t \to \infty) = \langle Z \rangle / (\epsilon_S{}^2 \langle S \rangle^2 + \epsilon_B{}^2 \langle B \rangle^2)^{1/2}, \quad (6)$$

where $\langle Z \rangle$, $\langle S \rangle$, and $\langle B \rangle$ are the mean numbers of photons due to zodi, star, and background, and ϵ_S and ϵ_B are the relative calibration accuracies, e.g., given by $\epsilon_B = (\langle B \rangle - \langle B \rangle^*)/\langle B \rangle$, where $\langle B \rangle^*$ is the estimate for $\langle B \rangle$. The limiting value for the SNR, determined by the calibration accuracy, is shown in the upper part of Fig. 5 for observing exo-zodiacal dust clouds of different strength (normalized to the strength of the local zodiacal dust cloud) around Sunlike stars at different distances from Earth. The SNR limit increases with increasing distance as the stellar leakage decreases. For large distances the SNR finally decreases because of the weak received signals, resulting in bad control loop performance. However,

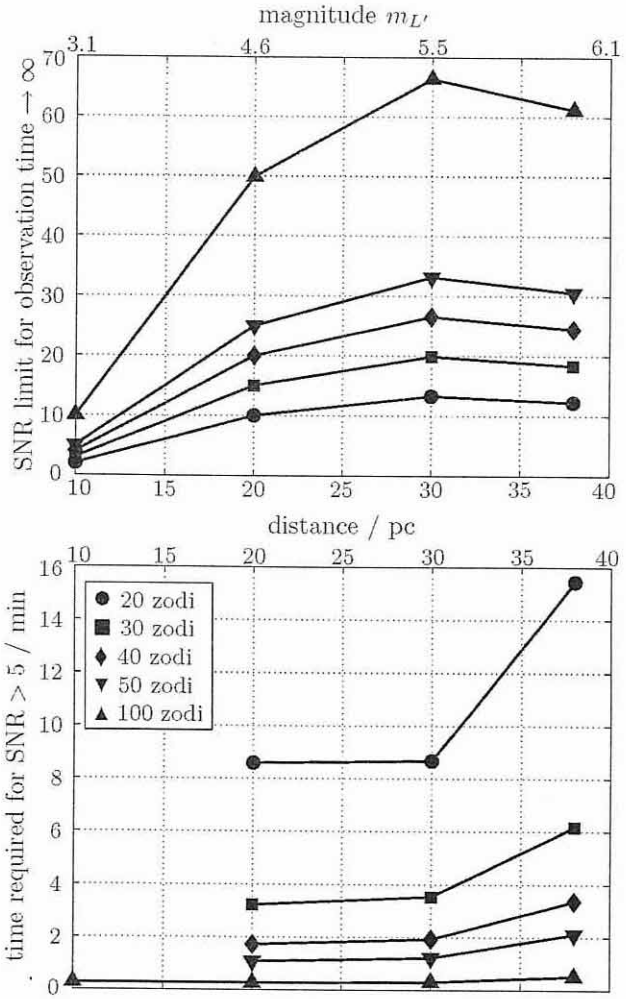

Fig. 5. Exo-zodiacal dust cloud observation performance of the proposed GENIE instrument for source scenarios at different distances from Earth. The upper part shows the SNR achievable for infinitely long integration times, the lower part shows the time required to achieve a SNR of at 5.

reasonably high values for the SNR may be achieved, at least for clouds at distances of 20 pc and larger.

The time required to achieve a certain value of SNR, which also depends on the photon noise, is dominated by transmission noise. The performance of the control loops (see Table 1) determines the temporal fluctuations of the received signals. Mainly the fluctuations of stellar leakage contribute to transmission noise and therefore affect the required integration time. Figure 6 shows the nulling ratio statistics, i.e., mean value and root mean square (rms), together with the theoretical nulling ratio for rejecting Sunlike stars at different distances from Earth. We define the nulling ratio R as the ratio of constructive interferometer output power to destructive interferometer output power, i.e.,

$$R = P_{\mathrm{constructive}}/P_{\mathrm{destructive}}. \quad (7)$$

The nulling ratio increases with increasing star–

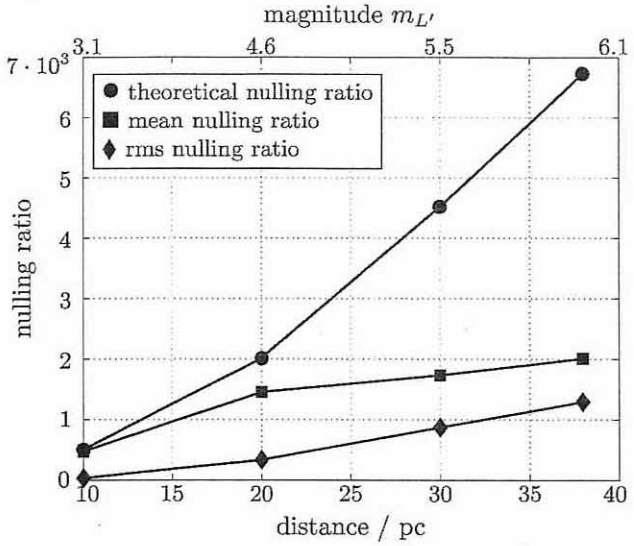

Fig. 6. Theoretical nulling ratio, mean nulling ratio, and the rms nulling ratio achieved with the GENIE instrument for Sunlike stars and hot-Jupiter planets at different distances from Earth.

Earth distance because of decreasing stellar leakage. The integration times required for achieving a SNR larger than 5 are shown in the lower part of Fig. 5. Even exo-zodiacal dust clouds as weak as 20 zodis can be observed within a few minutes. With increasing distance of the star from Earth, the integration time increases because of the decreased control loop performance.

One of the most critical parts for Earth-based interferometric observations is background calibration. Figure 7 shows the integration time required to achieve a SNR of more than five for detecting an exo-zodiacal dust cloud of 20 zodis around a star at different distances from Earth as a function of the background calibration accuracy. For the results shown in Fig. 5, a relative background calibration

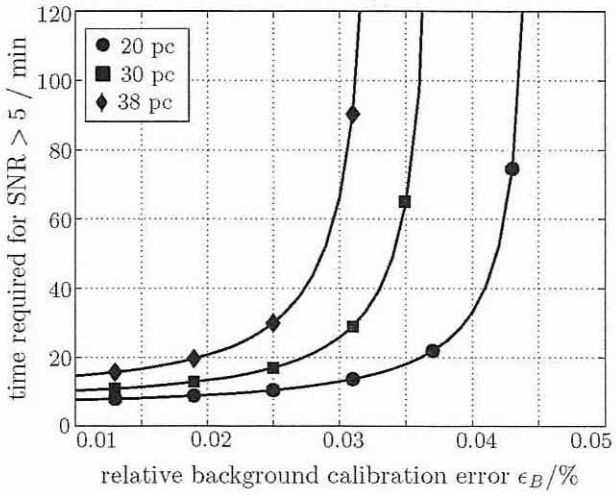

Fig. 7. Observation time required for detecting a 20-zodi dust cloud at different distances from Earth with a SNR of 5 as a function of the relative background calibration accuracy.

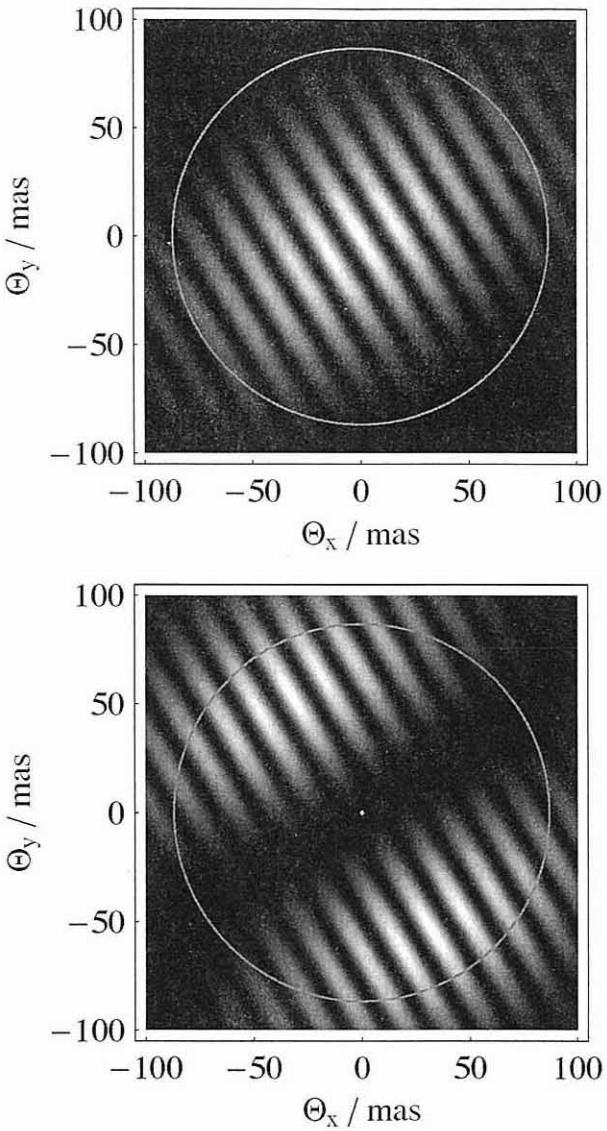

Fig. 8. Transmission maps of the UT2-UT3 split-pupil configuration for the detection mode (upper part) and for the calibration mode (lower part). The circles indicate the instrument's field of view.

accuracy of 0.01% has been assumed. This stringent requirement asks for high background stability within the instrument's FOV and for very low cross coupling between the fibers used for science measurements and that used for background measurements. If the required background calibration accuracy cannot be achieved, one may think of different instrument architectures allowing for better background subtraction. Almost perfect background calibration is possible with a split-pupil architecture,[5] where two subapertures are created for each of the telescopes UT2 and UT3, providing two modulation states, one, e.g., for exo-zodiacal dust cloud detection and one for background calibration. Figure 8 shows the transmission maps for the detection mode (upper part) and for the calibration mode (lower part).

We propose a novel concept where pupil splitting is

done after recombination, see Fig. 2 (note that two beams are arranged on top of each other). The big advantage is that only one set of control loops is required, and therefore the split-pupil architecture can be realized as an add-on to the conventional Bracewell architecture. In the simplest setup, even the internal laser metrology required for equalizing the paths within the split-pupil instrument may be omitted. However, the resulting additional OPD errors of typically 50 nm rms contribute to the transmission noise and therefore lead to integration times of several hours for achieving a SNR of 5. Our simulations showed that the maximum achievable SNR is identical to that achievable with the Bracewell configuration, and comparable integration times may be obtained with additional metrology.

5. Conclusions

We showed by simulation that weak exo-zodiacal dust clouds can be detected with a properly designed GENIE instrument.

Our proposed instrument is a Bracewell configuration utilizing UT2 and UT3, operates in L band, utilizes the VLTI instruments MACAO and (optionally) PRIMA FSU, and requires only four control loops for counteracting fluctuations of OPD, longitudinal dispersion, amplitude, and internal tip of tilt. A distinctive feature of the instrument is the OPD control with a fringe sensor operating within the science band. A pupil splitter, which can be inserted as an add-on, allows for modulation and thus for increased background calibration accuracy.

The proposed instrument is able to detect, within a few minutes of observation time, exo-zodiacal dust clouds around stars with a magnitude of 4.6 that are as weak as 20 times the density of the local zodiacal dust cloud. Calibration of stellar leakage and of infrared background turned out to be critical parameters for achieving a reasonably high SNR. Proper design of the instrument and optimization of the control loops is essential for reducing the transmission noise and therefore also the required integration time.

The work described was performed under ESA/ESTEC contract 17657/03/NL/HB by EADS Astrium GmbH (Germany) together with TNO-TPD (The Netherlands), Vienna University of Technology (Austria), Max-Planck Institute of Astronomy (Germany), and Observatory Leiden (The Netherlands). The authors are grateful to H. Bokhove, W. R. Leeb, U. Graser, A. Quirrenbach, and Ph. Gondoin (ESA/ESTEC).

References

1. M. Fridlund and Ph. Gondoin, "The Darwin mission," in *Interferometry in Space,* M. Shao, ed., Proc. SPIE **4852,** 394–404 (2003).
2. R. N. Bracewell, "Detecting nonsolar planets by spinning infrared interferometer," Nature **274,** 780–781 (1978).
3. Ph. Gondoin, O. Absil, M. Fridlund, Ch. Erd, R. den Hartog, N. Rando, A. Glindemann, B. Koehler, R. Wilhelm, A. Karlsson, L. Labadie, I. Mann, A. Peacock, A. Richichi, Z. Sodnik, M. Tarenghi, and S. Volonte, "The Darwin Ground-based European nulling Interferometry Experiment (GENIE)," in *Interferometry in Optical Astronomy II,* W. A. Traub, ed., Proc. SPIE **4838,** 700–711 (2002).
4. European Southern Observatory, www.eso.org/vlti (April 2005).
5. E. Serabyn, "Nulling interferometry progress," in *Interferometry in Optical Astronomy II,* W. A. Traub, ed., Proc. SPIE **4838,** 594–608. (2003).
6. Th. Herbst and Ph. Hinz, "Interferometry on the Large Binocular Telescope," in *New Frontiers in Stellar Interferometry,* W. Traub, J. D. Monnier, and M. Schöller, eds., Proc. SPIE **5491,** 383–390 (2004).
7. Ch. Leinert and U. Graser, "MIDI: the mid-infrared interferometric instrument for the VLTI," in *Astronomical Interferometry,* R. D. Reasenberg, ed., Proc. SPIE **3350,** 389–393 (1998).
8. E. Serabyn and M. M. Colavita, "Fully symmetric nulling beam combiners," Appl. Opt. **40,** 1668–1671 (2001).
9. J. Meisner and R. Le Poole, "Dispersion affecting the VLTI and 10 micron interferometry using MIDF," in *Interferometry in Optical Astronomy II,* W. A. Traub, ed., Proc. SPIE **4838,** 609–624 (2003).
10. T. Kelsall, J. L. Weiland, B. A. Franz, W. T. Reach, R. G. Arendt, E. Dwek, H. T. Freudenreich, M. G. Hauser, S. H. Moseley, N. P. Odegard, R. F. Silverberg, and E. L. Wright, "The Cobe Diffuse Infrared Background Experiment search for the cosmic infrared background II. Model of the interplanetary dust cloud," the Astrophys. J. **508,** 44–73 (1998).